BGSG

Volume 51

Research Paper

Correspondence to:
Athanassios Ganas
aganas@noa.gr

DOI number:
http://dx.doi.org/10.12681/bgsg.15004

Keywords:
Crete, Assimi earthquake, extension, seismicity, active fault

Citation:
Athanassios Ganas, Charalampos Fassoulas, Alexandra Moshou, George Bozionelos, George Papathanassiou, Christina Tsimi & SotirisValkaniotis (2017), Geological and seismological evidence for NW-SE crustal extension at the southern margin of Heraklion basin, Crete. Bulletin Geological Society of Greece, 51, 52-75.

Publication History:
Received: 21/11/2017
Accepted:4/12/2017
Accepted article online: 22/12/2017

The Editor wishes to thank two anonymous reviewers for their work with the scientific reviewing of the manuscript

Geological and seismological evidence for NW-SE crustal extension at the southern margin of Heraklion basin, Crete.

Athanassios Ganas[1], Charalampos Fassoulas[2], Alexandra Moshou[1], George Bozionelos[3], George Papathanassiou[4], Christina Tsimi[1] and Sotiris Valkaniotis[5]

[1]**National Observatory of Athens, Institute of Geodynamics,** aganas@noa.gr, amoshou@noa.gr, christinant@gmail.com
[2]**Natural History Museum of Crete, University of Crete,** fassoulas@nhmc.uoc.gr
[3]**National and Kapodistrian University of Athens, Dept. of Geology,** georgebozionelos@gmail.com
[4]**Aristotle University of Thessaloniki, Dept. of Geology,** gpapatha@geo.auth.gr
[5]**Koronidos Str., 42131, Trikala, Greece,** valkaniotis@yahoo.com

Abstract

We present new geological and seismological data on the orientation of crustal extension in central Crete (SE Heraklion basin) following the occurrence of two shallow seismic sequences: a) the May 2005 Assimi Mw=4.1 and b) the 2013 Houdetsi-Tefeli sequence (3.2≤Mw≤3.6). Emphasis is given to the results of the geological field work, stress analysis of slip vector data, source inversion, aftershock relocations and mapping of earthquake-induced effects. For the first time we find seismological evidence for N-S strike-slip motions along shallow, near-vertical fault planes in central Crete (Amourgeles fault). Our results indicate that while crustal extension dominates there is a combination of active fault kinematics, ranging from NE-SW normal faulting along the northern edge of Messara basin (south-dipping Plakiotissa fault) to N-S strike-slip faulting inside the SE Heraklion basin (Houdetsi-Tefeli). The combination of active fault motions accommodates a NW-SE extension of the upper crust.

Keywords: *Crete, Assimi earthquake, extension, seismicity, active fault*

Περίληψη

Στην εργασία αυτή παρουσιάζονται νέα γεωλογικά και σεισμολογικά δεδομένα σχετικά με τον προσανατολισμό του εφελκυσμού του στερεού φλοιού στην κεντρική Κρήτη. Τα δεδομένα προέρχονται από γεωλογικές χαρτογραφήσεις και ανάλυση της σεισμικότητας στην περιοχή της Ανατολικής Μεσσαράς – νοτιοανατολικής λεκάνης του Ηρακλείου, όπου σημειώθηκε ο σεισμός Μ4.1 τον Μάϊο του 2005 και η σεισμική ακολουθία του 2013. Αναλυτικότερα παρουσιάζονται τα εξής: γεωλογικός χάρτης με σημειωμένα τα ενεργά ρήγματα, υπολογισμός των τεκτονικών τάσεων από μετρήσεις ανυσμάτων ολίσθησης, υπολογισμός του τανυστή σεισμικής ροπής με την μέθοδο της αντιστροφής, επαναπροσδιορισμός των επικέντρων της σεισμικής ακολουθίας του 2013 και χάρτης με τις δομικές βλάβες του σεισμού του 2005. Για πρώτη φορά τεκμηριώνεται η ύπαρξη ενεργού ρήγματος οριζόντιας ολίσθησης με δεξιόστροφη συνιστώσα στην κεντρική Κρήτη (ρήγμα Αμουργελέ). Τα αποτελέσματα αυτής της εργασίας δείχνουν ότι για να δράσει ο βορειοδυτικός-νοτιοανατολικός εφελκυσμός στην κεντρική Κρήτη χρειάζεται συνδυασμός τεκτονικών κινήσεων, δηλαδή η σύγχρονη ενεργοποίηση κανονικών, βορειοανατολικών-νοτιοδυτικών ρηγμάτων και ρηγμάτων οριζόντιας ολίσθησης με διεύθυνση βορρά-νότου.

Λέξεις κλειδιά: *Κρήτη, σεισμός Ασήμι, ενεργά ρήγματα, σεισμικότητα*

1. Introduction

Crete lies in a prominent position in the fore-arc of the Hellenic Subduction Zone, i.e. near the shallow portion of the presently active region of plate convergence where large earthquakes are most likely to occur (Delibasis et al., 1981; Drakopoulos et al., 1983; Ganas and Parsons, 2009; Kiratzi, 2016; Papadimitriou et al., 2016). In contrast to a converging tectonic regime at depth, the upper crust of Crete displays numerous evidence of extensional deformation along both arc-parallel, high-angle, E-W striking faults and along arc-normal, high-angle pure-normal and oblique-normal faults that strike on average N-S (e.g. Ten Veen and Meijer, 1998; Papanikolaou and Nomikou, 1998; Fassoulas, 2001 and references therein; Caputo et al., 2010; Ganas et al., 2010; Ganas et al., 2011; Mason et al., 2016). Sets of possibly-active normal faults striking NW-SE and NE-SW occur inside the Heraklion basin, as well (Fig. 1; Fassoulas, 2001; Ganas et al., 2010; 2011; Zygouri et al., 2016).

Several marine basins were formed onshore (present-day) Crete due to crustal extension since late Miocene, striking in two prominent orientations, east-west and north-south

(Fassoulas et al., 2001). The largest is the Messara basin (Fig. 1) located at the south Heraklion province, bordered to the north by the Psiloritis Mountains and the Heraklion basin uplands and to the south by the Asteroussia Mountains. The Messara basin was initiated in Early Pliocene due to east-west striking normal faults that uplifted gradually the northern part of the former Heraklion basin and subsided the central part of the Messara basin (Meulenkamp et al., 1979, 1994). Several studies have documented that active normal faulting occurs in the western part of the basin (Delibasis et al., 1981; Ten Veen and Kleinspehn, 2003; Peterek and Schwarze, 2004). However, the onshore active-tectonic setting of the eastern Messara area, including the south (lower) part of Heraklion basin (of Tertiary age – Vidakis et al., 1996) remains poorly known (e.g. Ten Veen and Meijer, 1998; Fassoulas 2001).

The goal of this paper is to present new geological and seismological data on the orientation of crustal extension following the occurrence of two shallow seismic sequences in eastern Messara – Heraklion basin border area (central Crete; Fig. 1). In particular, we present results on a) the May 2005 Assimi earthquake, and b) the 2013 Houdetsi-Tefeli sequence (see Fig. 1 for epicentre locations). The orientation of crustal extension is of great importance in terms of seismic hazard for the city of Heraklion, as it constrains the orientation of optimal normal faults; there are both N-S and NE-SW striking normal faults with evidence for Quaternary activity. We first present new geological data on active faulting in the greater area of Assimi – Plakiotissa villages. Then we present seismological data (moment tensor inversion of the 2005 and 2013 main events, relocation of the 2013 seismic events) in order to map shallow seismicity and document the orientation of the least principal stress axis. We discuss our findings in view of seismic hazard assessments for the city of Heraklion and in terms of onshore upper plate strain.

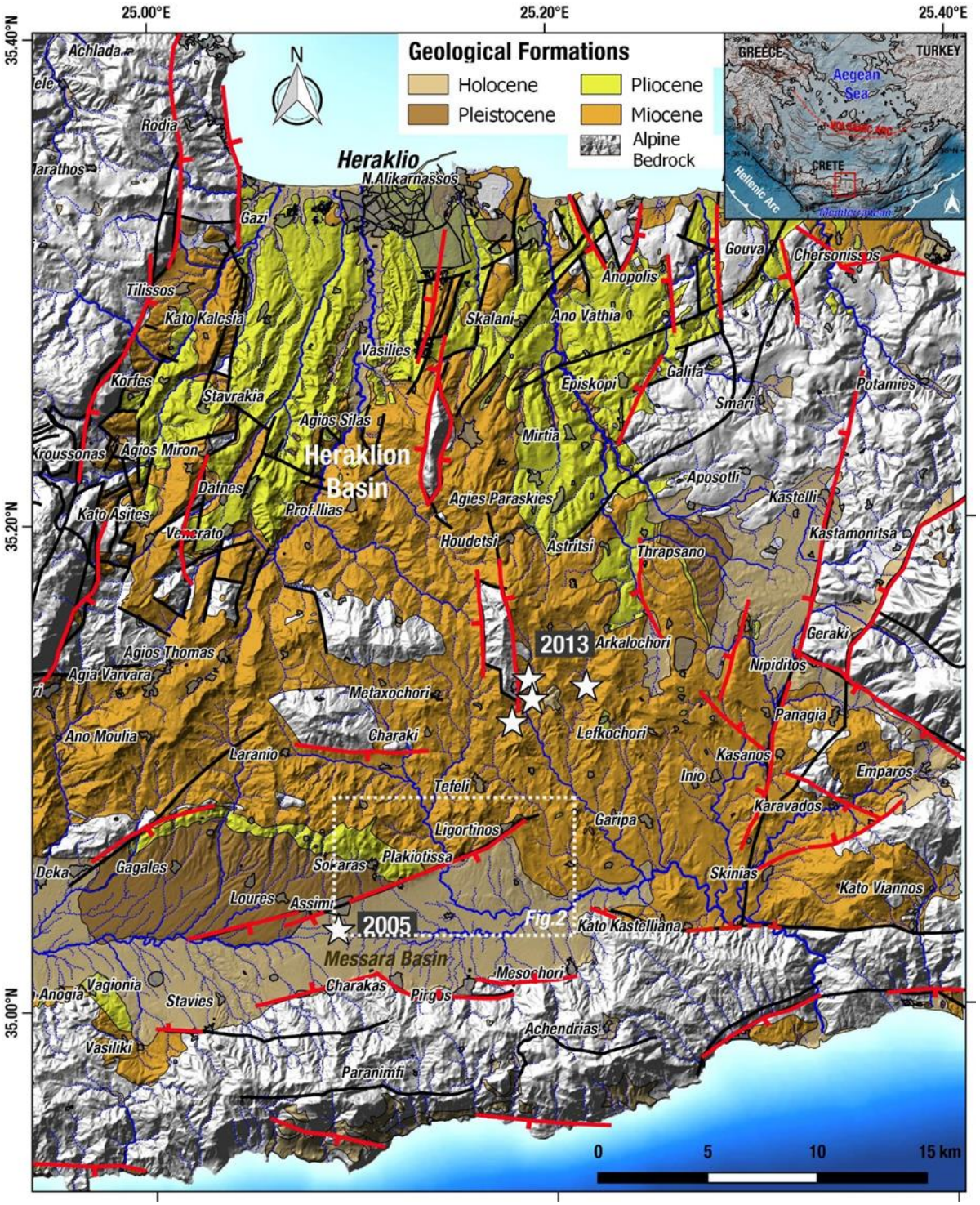

Fig.1. Geological map of central Crete showing active faults and epicentres of the 2005 and 2013 earthquakes, respectively. Geology was compiled from published geological maps sheets of IGME (i.e. Heraklion, Epano Archanae, Timpakio and Akhendhrias; Vidakis et al. 1994, Papavassiliou et al. 1984a, b, and Katsamangos et al. 1996). Red lines with ticks represent active faults (ASPIDA project and this study). Black lines are IGME faults. Dotted white box indicates extent of Figure 2.

2. Geological setting – Data analysis

Our study included field mapping (at 1:5000 scale – map in Fig. 2) of the Late Quaternary deposits that crop out along the Assimi and Plakiotissa areas of eastern Messara, around the mapped normal fault of Vidakis et al., (1994), and collecting observations on the geomorphological context (in the field and on 1:5000 scale topographic diagrams of the Hellenic Army Geographical Service). The outcrop of the contact near Plakiotissa which is interpreted as an active fault juxtaposing Quaternary against Neogene deposits was cleaned thoroughly and examined in situ.

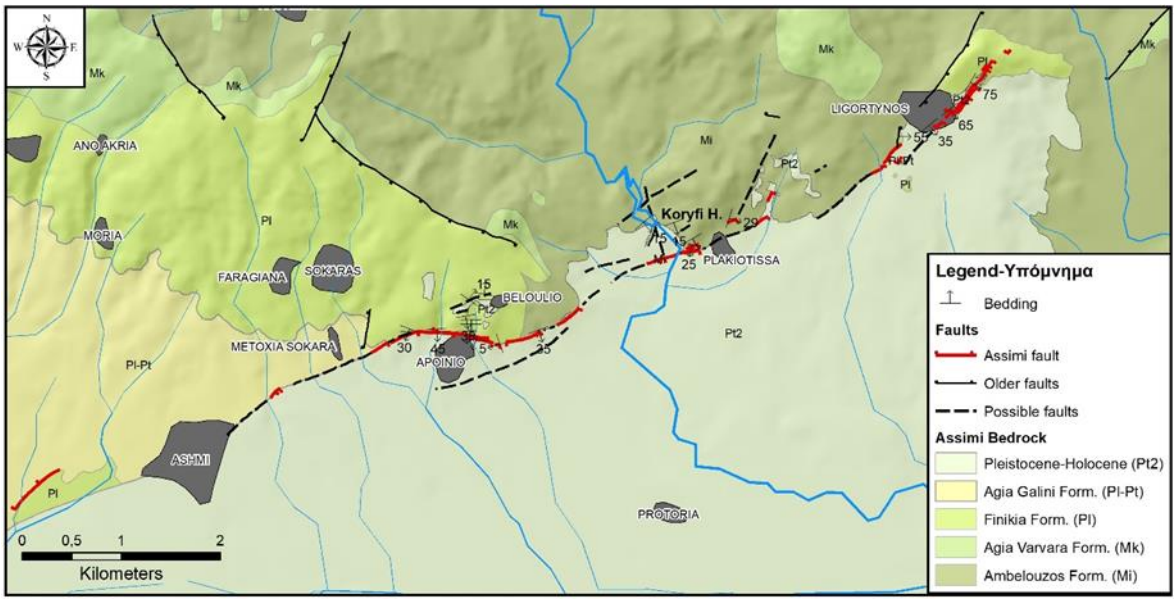

Fig. 2. Geological map of the Assimi area, central Crete. Active faults are shown in red.

In the geological map of 1:50000 of IGME Epano Archanae sheet (Vidakis et al., 1994) a long normal fault, striking NE-SW and dipping to the south was mapped juxtaposing the Pleistocene to Holocene fluvial lacustrine deposits. The latter cover the central part of the basin with the Pliocene-Pleistocene deposits of Agia Galini formation occurring at its western part while other Neogene deposits occur at its eastern part. Field work was conducted several weeks after the 2005 Assimi earthquake and was focused on this fault aiming to map in detail the fault outcrops, to identify existing fault scarps and to study the microstructural and kinematic setting of the fault zone (Fig. 2). No evidence of fault reactivation due to the Assimi earthquake were found in the study areas, as it was expected due to the moderate magnitude of this event (M_L=4.0) where the rupture did not reach the ground surface.

Fault surfaces were identified in several locations especially near the villages of Ligortinos to the east, Plakiotissa and Apoini to the west (Fig. 2). The normal fault has

created a fracture zone of several tens of metres which in some places appears as a striking morphological scarp of 10 to 20 metres height. In the area of Ligortinos (Fig. 2) the fault was mapped just south and east of the village with a NE-SW strike. Two parallel fault planes juxtapose the lower Pliocene deposits of *Finikia* Formation, that comprise of white to light gray marls, with the Pleistocene-Holocene fluvio-lacustrine deposits of the basin that contain also fragments of pottery. An offset of the Pleistocene-Holocene deposits ranging from 1 - 3 m has been measured. The fault appears to disperse to the northeast of the village making difficult its identification. In this area an antithetic fault striking NE-SW with slickensides, has been mapped. Hydrogeological studies and water drillings in Messara basin (Kritsotakis, 2009) have shown that in the area south of Ligortinos, the Assimi-Plakiotissa normal fault is responsible for a net vertical offset of the Pleistocene-Quaternary deposits of about 55 m.

Sparse fault scarps were mapped between the area of Ligortinos and Plakiotissa villages (Fig. 2). In that area the fault juxtaposes Upper Tortonian-Messinian alternations of marine, brackish and fluvial conglomerates, sandstones, siltstones and clay of the *Ambelouzos* formation with the Pleistocene-Holocene conglomerates. The most outstanding outcrop of the Assimi fault occurs in the ravine, west of Plakiotissa village (Fig. 3). The fault develops with at least three major fault surfaces, the upper one existing at the foot of the Koryfi hill, just north of the settlement (see Fig. 2 for location). This surface juxtaposes the Miocene *Ambelouzos* deposits with the Pleistocene-Holocene conglomerates and is the major structure prevailing in the landscape. The fault at this area strikes almost E-W, dipping with 75-80o to the south. The fault scarp is formed by a cataclastic zone of about 30 cm, a cemented crust exposing slickensides, steps and other kinematic indicators of a normal sense of shear (Fig. 3).

Along the fault scarp a fault gouge of about 2 m is formed by both the Miocene and Quaternary deposits (Fig. 3; Fig. 4). Smaller fault zones with the same geometric features, Reidel shears and asymmetric boudins also indicate a normal sense of shear within this gouge zone. A second, parallel to the major one, fault plane juxtaposes the gouge with the Pleistocene-Holocene deposits that extent further to the south. An antithetic fault surface with numerous slickensides dipping at about 75° to the north was identified just 10 m towards the river bed. A third, parallel fault plane, within the Pleistocene-Holocene deposits occurs about 15 m southwards, just at the stream side, without clear kinematic or shear indicators.

Fig.3. Field photograph of the fault scarp west of Plakiotissa, Messara, Crete. Left (view to the NE), right: view of the polished fault plane.

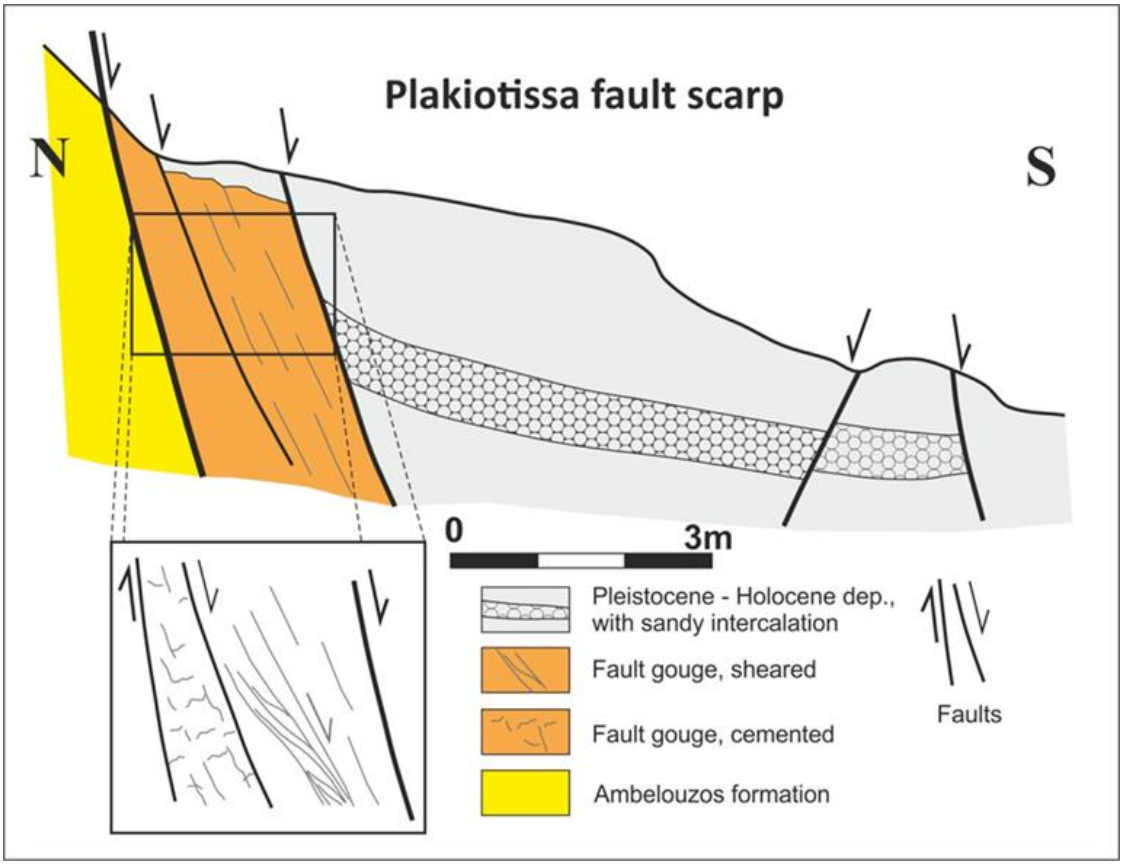

Fig.4. Schematic cross-section across the Assimi fault near the Plakiotissa locality.

It is remarkable that in this area the geomorphological study of the hydrographic network reveals a dextral offset of the main Plakiotissa stream of about 80 m (Fig. 2), where a small earth dam exists. At the footwall, the stream runs NW-SE, whereas at the hanging wall approximately N-S, which is presumably due to recent tectonic activity along the fault. The Assimi-Plakiotissa fault zone extends further to the west towards the villages of Apoini and Assimi, changing in places orientation from east-west to northeast-southwest. Traces and indications of the fault scarp have been found in few places. The most characteristic occurs just south of the Apoini village (Fig. 2). There, the fault zone runs again at the feet of the nearby hills forming two well-formed triangular facets on its footwall. Again, the fault is oriented E-W and occurs in two parallel planes that dip 70-75° to the south. The fault juxtaposes the Pliocene *Finikia* formation with the Pleistocene-Holocene conglomerates. In this area the conglomerates have been also mapped in a small half-graben that exists over the hills of the footwall. A total vertical offset (throw) of 60 m was estimated for these Holocene deposits. The fault near the village of Assimi (Fig. 2) becomes invisible as it enters into the Messara plane and the intensely cultivated area. In one outcrop east of the village a fault scarp was observed striking NE-SW and dipping at about 50° to the south. It juxtaposes the Miocene *Ambelouzos* formation with the Pleistocene-Holocene conglomerates which show an offset of about 1 m. However, hydrogeological studies in the area indicate a net vertical offset of the Holocene deposits of about 40 m (Kritsotakis, 2009). Apart from the Assimi fault several other, possibly older faults have been identified running either parallel to the Assimi or at an oblique direction. Some other minor faults developed along the E-W orientation (Fig. 2) have been also mapped. North of Plakiotissa one such fault with lateral movement was studied. The fault occurs within the *Ambelouzos* formation with moderate dip-angles.

The paleostress inversion analyses of the Plakiotissa locality fault planes (23 data points) indicated a tension axis (T) at moderate angles along the NNW-SSE orientation (N12°W; Fig. 5). We have used the *FaultKinWin* application (a program for analyzing fault slip data for Windows computers by R. W. Allmendinger; Allmendinger 2001) in order to analyze fault surface and kinematic data, extract the P and T dihedra and reconstructing paleostress axes.

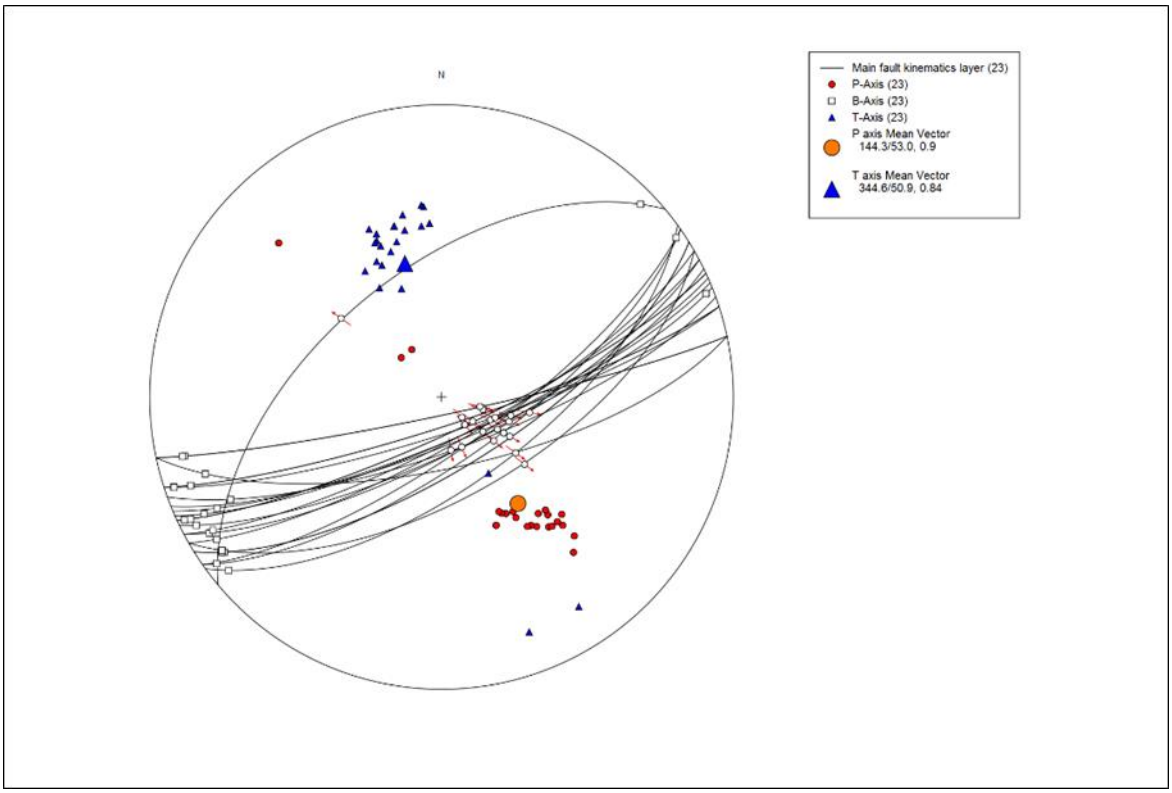

Fig.5. Lower hemisphere, equal area projection of measured shear surfaces and their kinematic characteristics from Assimi fault. Triangles show tension and cycles pressure stress axis for each surface, whereas larger symbols show the mean stress-inversion values for Assimi fault, using the dihedral area stress inversion method.

3. The 2005 Mw4.1 Assimi earthquake

The 2005 Assimi earthquake was a shallow moderate event that occurred on 1st May 2005 at 20:46 UTC with local magnitude M_L(NOA)=4.0 (its epicentre was determined by NOA at 35.03° N - 25.09° E; Fig. 1). The moment tensor solution for the mainshock was provided by E. Sokos (UPSL, Fig. 6; M_w=4.1). This event is also reported with M_w=4.1 in the catalogue of Makropoulos et al., (2012). The weeks following this earthquake, we conducted field work and collected structural data during spring and summer 2005 (Fig. 1, 2; mapping by ChF and AG), we compiled a map of building damages in Assimi (Fig. 7; data collected by GP on 8 July 2005) and surrounding villages. The mainshock was followed by a short (two-week) aftershock sequence with a general NE-SW orientation. The mainshock caused some structural damage in Assimi, as well as in the villages Apoini and Sokaras. In total we mapped 55 cases of small (light) damage to buildings (Fig. 7; mainly contained in the walls without affecting structural elements).

The focal mechanism was obtained by applying the ISOLA software (http://seismo.geology.upatras.gr/isola/ ; Sokos and Zahradník, 2008; Fig. 6) and shows two almost E-W striking fault planes with normal sense of slip. The magnitude of the earthquake was determined at M_w=4.1 and its centroid depth at 4 km. Despite the errors in hypocentre location (2-3 km; average in depth and horizontal error) due to the limited number of seismic stations on Crete during 2005, we propose that the seismic fault is the normal fault outcropping in the area of Assimi-Plakiotissa villages (Fig. 2), as the nodal plane of the MT solution 85°/46°/-80° (strike/dip/rake) is compatible with our field measurements. Therefore, the Assimi-Plakiotissa fault is an active normal fault bordering the Messara plain, strikes NNE-SSW, dips to the south and its kinematics are in agreement with the obtained MT solution for the 2005 earthquake.

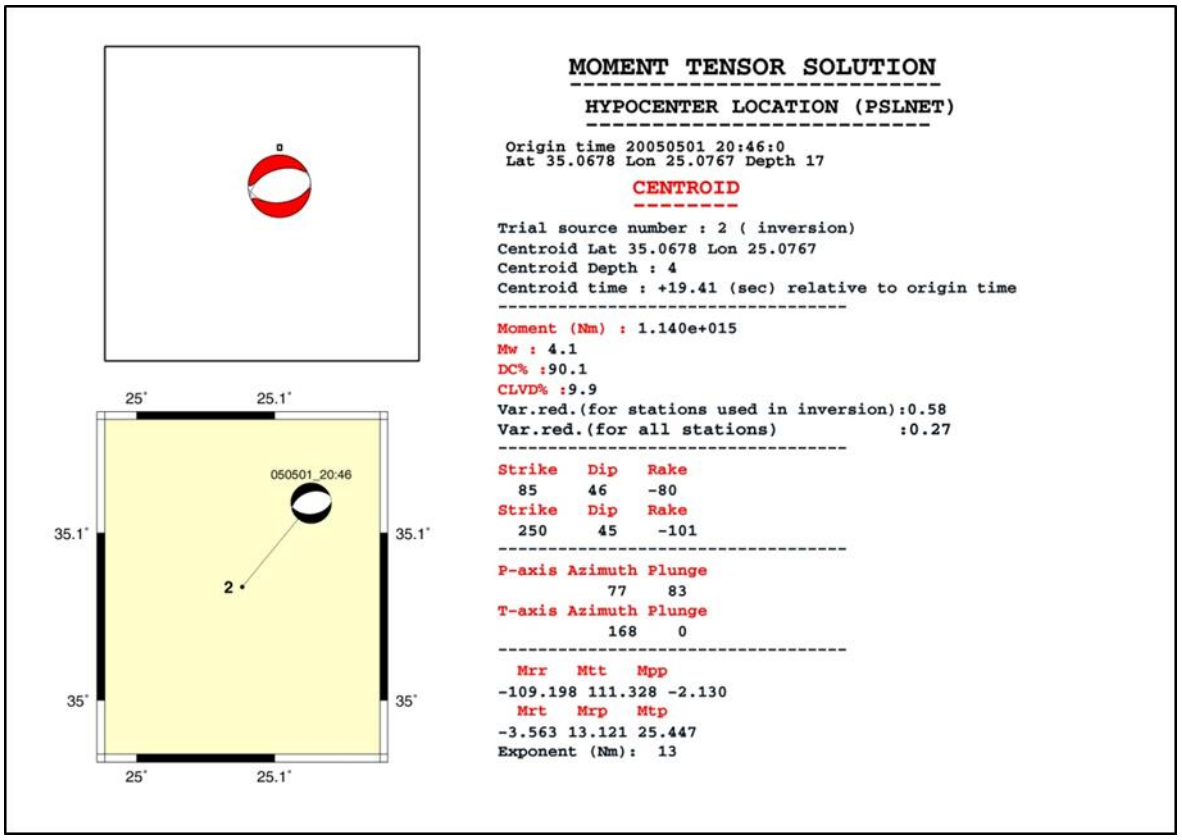

Fig.6. Focal place solution of the May 1st, 2005 earthquake (Mw=4.1). Solution provided by Efthimios Sokos, UPSL.

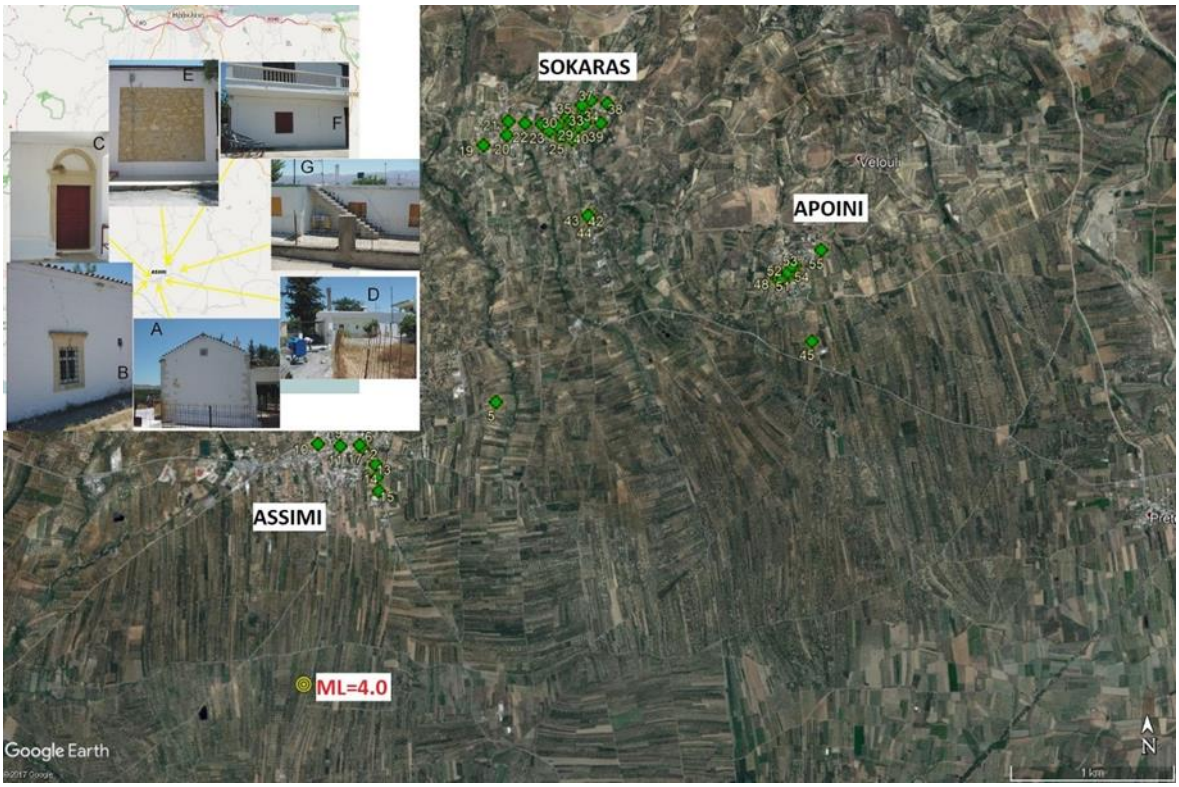

Fig.7. Google Image map showing localities with building damage (green symbols) and mosaic of field photographs from light damages in buildings (houses, church etc.) following the 1 May 2005 M_w4.1 earthquake (yellow circle).

4. The 2013 Houdetsi – Tefeli seismic sequence

4.1 Relocation of seismic events

The 2013 Houdetsi – Tefeli sequence occurred along a NNW-SSE strike-slip fault, as it was revealed by relocation of seismicity data and moment tensor inversion (Figures 8 & 9; Table 1; MT analysis conducted by AM; relocation conducted by GB). From the spatial distribution of the seismic sequence, it is evident that it extends from the area south of the village Houdetsi up to village Tefeli (Fig.1; Fig. 8; about 10 km long). The 2013 sequence occurred 7 km to the northeast of Assimi so it is interesting to investigate its properties, including geometry and kinematics of the seismic fault. The sequence started on April 11, 2013 with the largest event occurring on 22 April 2013 14:11 UTC (M_L=3.4 – M_w=3.6).

The algorithm used for event relocation follows the probabilistic formulation of nonlinear inverse problems by Tarantola and Valette (1989) providing a complete probabilistic solution expressed in terms of a posterior density function (PDF). To the likelihood function, Equal Differential Time approximate (EDT) is selected that is much more robust in the presence of outliers. Oct-Tree Importance sampling algorithm

approach was used to compute the PDF (Lomax and Curtis, 2001). Regarding the number and chronology of events, 115 earthquakes were recorded by the Hellenic Unified Seismological Network (HUSN) and the Seismological Network of Crete for the period 13-03-2010 to 12-07-2014 (in this analysis we include only the 2013 events). While the catalogue from National Observatory of Athens included P- and S- arrivals from HUSN stations, we enriched these data adding the phases from Seismological Network of Crete in order to achieve better accuracy. The phases from both networks were united and the initial events were relocated, applying the nonlinear location algorithm *NonLinLoc* (Lomax et al., 2000; Fig 8). All relocated events comprise at least 4 P- and 2 S-wave manually determined arrivals.

Several local velocity models, that were previously determined for the region by other studies, were tested so as to obtain the best possible hypocentral accuracy. In order to assess the quality of the hypocentral location determination, histograms with the RMS error, the spatial errors, and the maximum half-axis (LEN3) of the 68% confidence ellipsoid are created and evaluated (see Fig. 10 for histogram plots). The adopted Oct-Tree sampling method allows the representation of the location uncertainties by density plots. These scatter plots are obtained by drawing samples from the probability density function (PDF) with the number of samples proportional to the probability (Lomax et al., 2000). The form of the distribution of the scatter points is indicative of the quality of the solution and it is examined along with the difference between the maximum likelihood and expectation location for each event (Lomax et al., 2000). Uncertainty introduced during phase manual determination, both as a factor of noise presence and as miss pick of *Pn* phase as *Pg* at more distant stations, is a common issue in catalogues. As an additional procedure, the travel-time residuals were examined separately for each station as a function of the epicentral distance to assess the validity of the picks.

Finally, cross sections were drawn perpendicular to the long-axis of event distribution (the ENE-WSW section is shown in Fig. 9; it is noted as a-a' in Fig. 9) and the spatial distribution of the foci is “imaged” and compared with the possible activated fault structures (Fig. 1; Fig. 9). The best results were derived using the velocity model of Becker et al., (2010). Table 1 depicts the location and depth of the four (4) main events of the sequence (origin time and local magnitude data from the NOA online database http://bbnet.gein.noa.gr/HL/databases/database). The limited azimuthal coverage and the small number of phases in nearby stations, is reflected on the relatively high values of the errors. Besides that, the resulting hypocentral distribution indicates the activation of a nearly N-S shallow, near-vertical fault with hypocentral depths ranging between 3-15 km.

Table 1. Earthquake parameters of the main events of the 2013 Houdetsi sequence as determined by relocation. Local magnitude is from NOA catalogue, moment magnitude was determined in this study.

No	Origin Date	Origin Time	Latitude	Longitude	Depth (km)	M_L	M_w
1	2013-04-22	14:11:50	35.1308	25.1865	8.0	3.4	3.6
2	2013-04-22	15:49:47	35.1340	25.1838	4.0	3.1	n/a
3	2013-04-23	10:00:04	35.1358	25.1840	5.1	3.2	3.4
4	2013-12-02	06:17:03	35.1325	25.1853	4.0	3.1	3.3

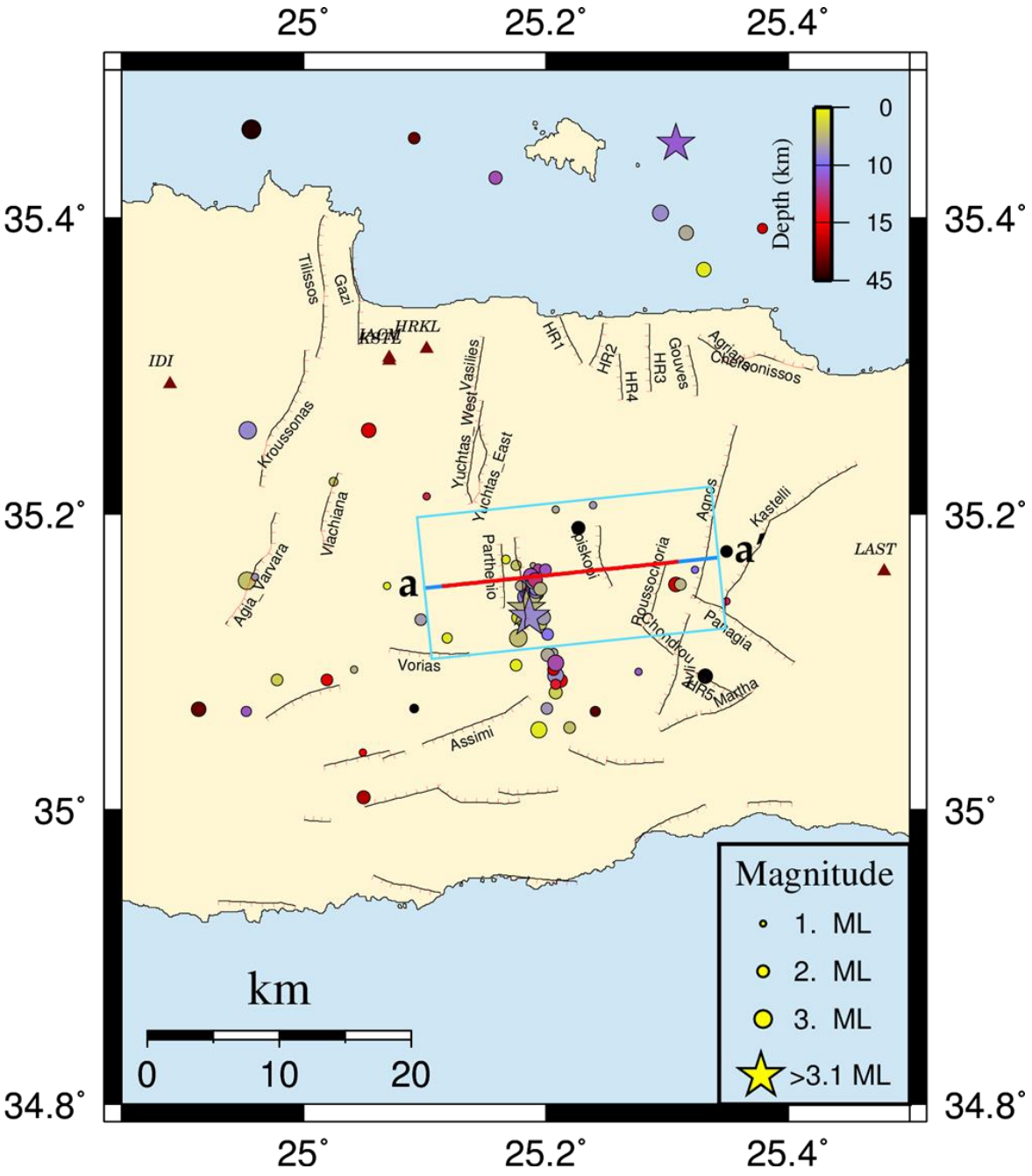

Fig.8. Seismicity map of central Crete showing relocated events. Note the NNW-SSE arrangement of shallow seismicity. Grey lines with ticks indicate normal faults of the ASPIDA project (unpublished data) as well as the Assimi fault (this study). Triangles indicate seismological stations. Section a-a' is depicted in Fig. 9.

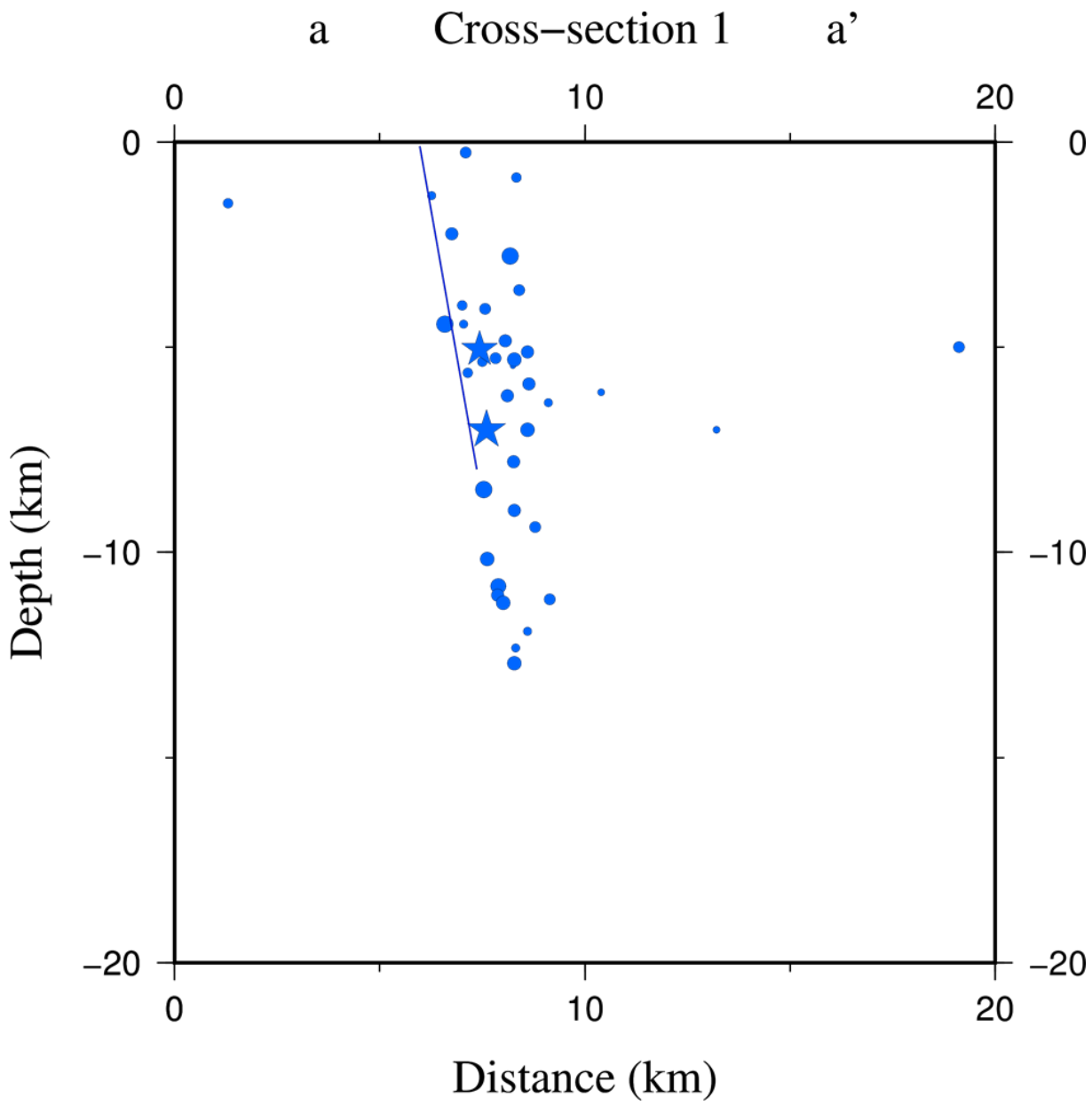

Fig.9. WSW-ENE, vertical cross section of relocated events. A near-vertical fault plane is inferred (thin blue line) that was activated during the 2013 sequence.

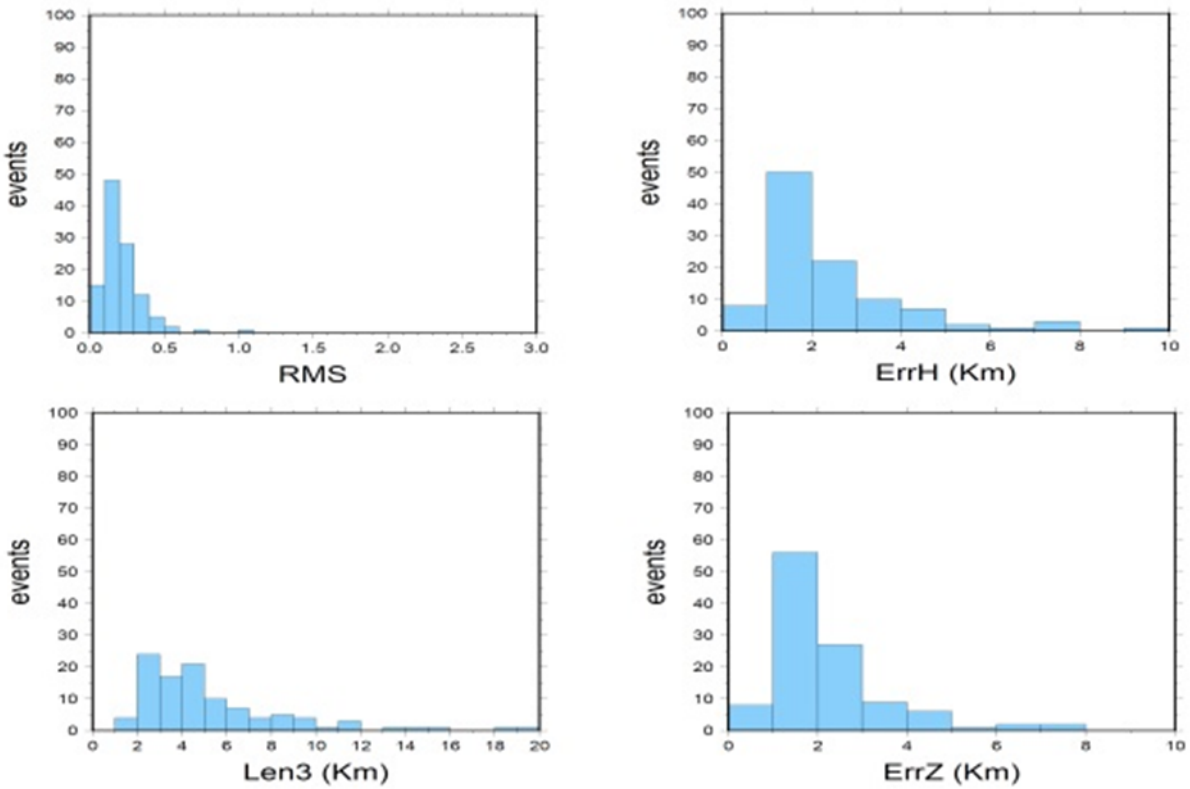

Fig.10. Histograms showing statistics of relocation: (top left) RMS error (in seconds), (top right) horizontal error in km, (bottom right) vertical error in km and (bottom left) maximum half-axis (LEN3) of the 68% confidence ellipsoid.

4.2 Moment Tensor Inversion

Seismological broadband data from HUSN were collected and analyzed in order to determine the source parameters of the 2013 events that occurred in central Crete. For this purpose, a methodology based on a moment tensor inversion was used. Data of 10 broadband stations equipped with three components seismometers (Fig. 11), HUSN were selected and analyzed. All stations are located at epicentral distances between 26 and 105 km except for station APE that is located 217 km to the North. APE was not important for the inversion but it contributed with data that were considered useful for the final quality of the solutions.

The source parameters of four earthquakes with magnitudes $3.2 \leq M_w \leq 3.6$ were calculated (Table 2; Fig. 12) using regional waveforms at epicentral distances less than 3°. Usually we use at least four stations at different azimuth coverage and with an epicentral distance not more than 200 km. The preparation of the data, includes the

deconvolution of instrument response, integration to displacement and rotation of the horizontal components to radial and transverse.

The reflectivity method of Kennett (1983) as implemented by Randall (1994) was applied to determine the Green Functions. The 3-D velocity model proposed by Papazachos (1998) was used. Initially Green's functions for different depths were calculated. Initial inversions were performed at a depth interval of 5 km followed by a finer one every 1–2 km around the depth that exhibited the lowest misfit. A band pass filter is applied to both the observed waveforms and synthetics. We used a frequency band between 0.05Hz – 0.02Hz although the magnitudes were in the range $3.2 \leq M_w \leq 3.6$. In all our inversions we use a fixed waveform length of 80 seconds (the results of the inversion indicate that inverting waveforms longer than 80 seconds resulted in higher misfits). The quality of the results of moment tensor solutions can be evaluated by considering the average misfit and the compensated linear vector dipole (CLVD; Table 2). For each solution there is a quality code that consists between the letters A – D, for the minimum misfit and between the numbers 1 – 4 for the percent of CLVD (Konstantinou et al., 2010; Fig. 12).

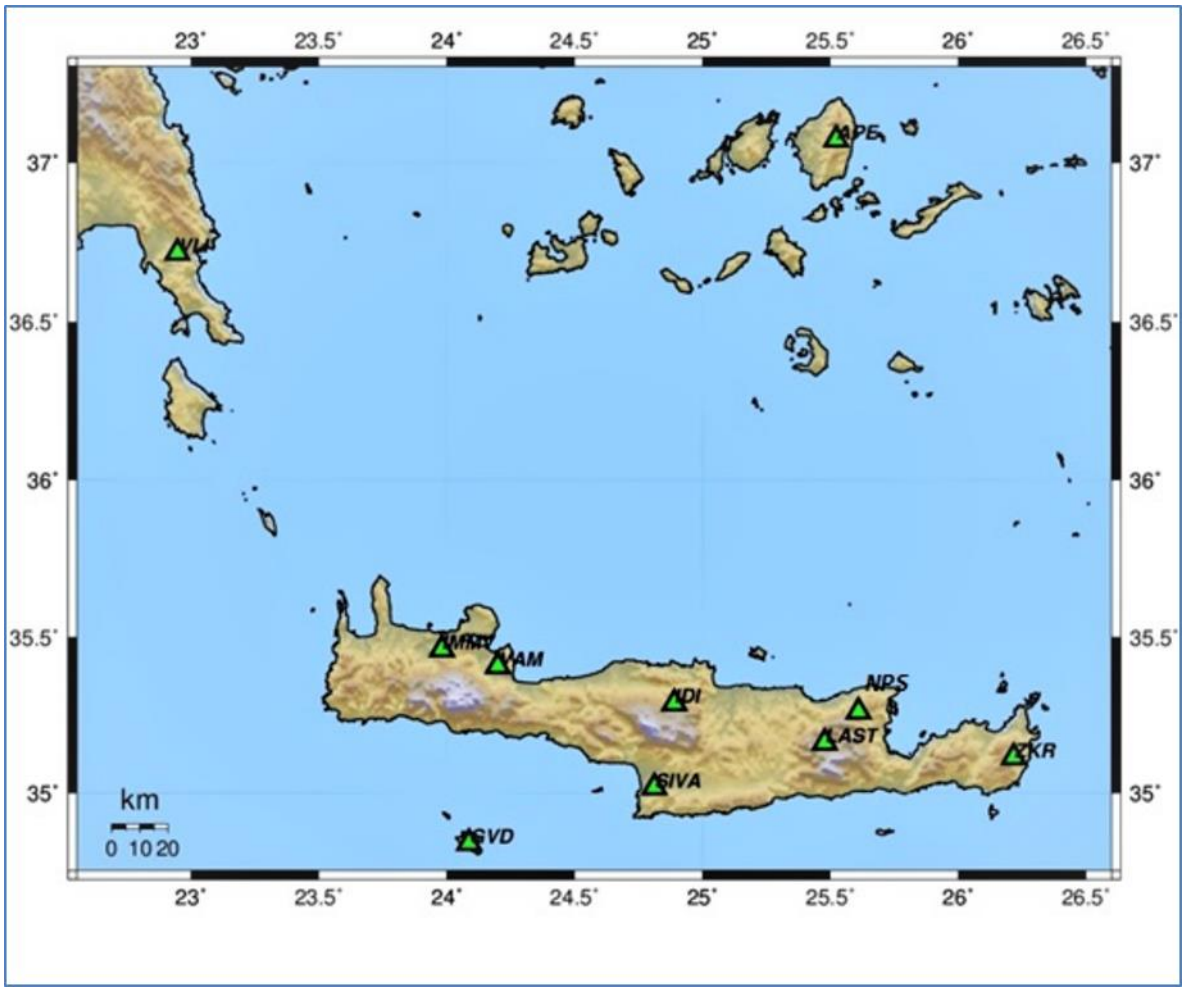

Fig.11. Maps showing location of seismic stations (green triangles) used in the moment tensor inversion of the 2013 sequence.

Table 2. Fault plane solutions of the main events determined by moment tensor inversion. All solutions are strike-slip with high percentage of a double-couple source. Column Mo indicates seismic moment (in dyn-cm). Column DC indicates the percentage of the double-couple source mechanism (or only shear motion on the fault plane). Column misfit is a quality estimate of the MT inversion, representing average waveform misfit. A map with contributing stations is shown in Figure 11.

Origin Time		Nodal Plane 1			Nodal Plane 2			Magnitude		DC	Misfit
Date	Time	Strike (°)	Dip (°)	Rake (°)	Strike (°)	Dip (°)	Rake (°)	M_0	Mw		
20130411	18:49:14.23	353	70	167	87	78	19	0.647e+21	3.2	86.4	0.67
20130422	14:11:50.12	9	68	152	110	64	24	0.289e+22	3.6	97.6	0.49
20130423	10:00:04.80	7	70	156	106	68	22	0.131E+22	3.4	97.6	0.49
20131202	06:17:03.50	16	69	165	112	70	22	0.647e+21	3.3	97.6	0.49

Fig.12. – continued next page: Moment tensor solutions of the 2013 earthquakes in central Crete. To the left observed and synthetic displacement waveforms (continuous and dotted lines respectively) are shown, at the inverted stations for the radial, tangential and vertical components. At the right part of the figure the summary of the solution and the fault plane solution as lower hemisphere equal area projection, are depicted. a) Moment tensor solution of the 20130411 (Mw=3.2) earthquake b) Moment tensor solution of the 20130422 (Mw=3.6) earthquake c) Moment tensor solution of the 20130423 (Mw=3.4) earthquake and d) Moment tensor solution of the 20131202 (Mw=3.3) earthquake, respectively.

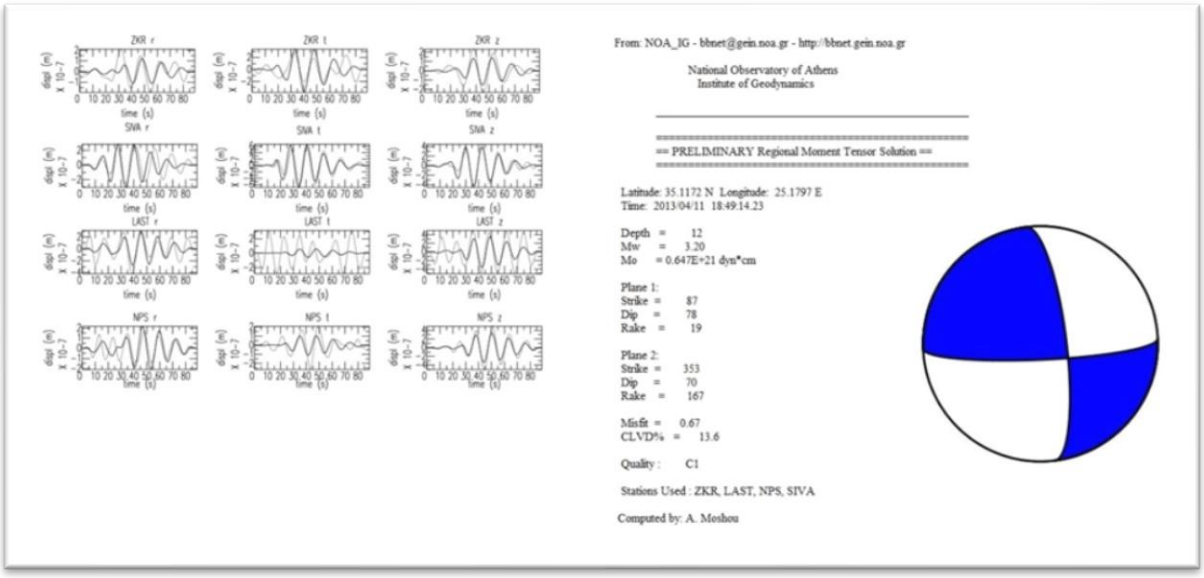

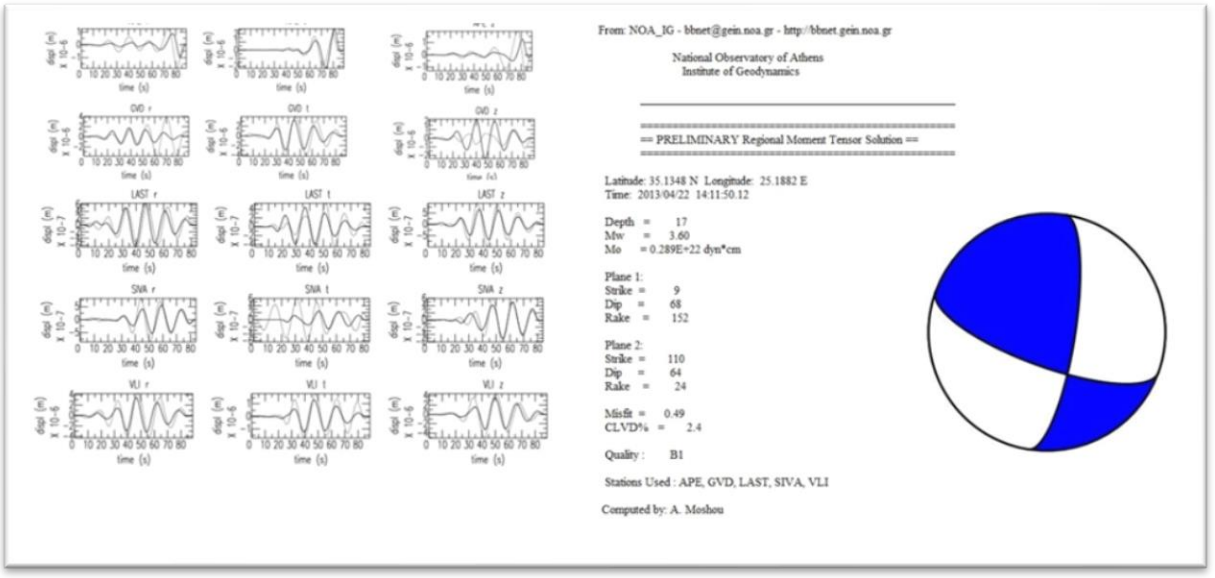
From: NOA_IG - bbnet@gein.noa.gr - http://bbnet.gein.noa.gr
National Observatory of Athens
Institute of Geodynamics
== PRELIMINARY Regional Moment Tensor Solution ==
Latitude: 35.1348 N Longitude: 25.1882 E
Time: 2013/04/22 14:11:50.12
Depth = 17
Mw = 3.60
Mo = 0.289E+22 dyn*cm
Plane 1:
Strike = 9
Dip = 68
Rake = 152
Plane 2:
Strike = 110
Dip = 64
Rake = 24
Misfit = 0.49
CLVD% = 2.4
Quality : B1
Stations Used : APE, GVD, LAST, SIVA, VLI
Computed by: A. Moshou

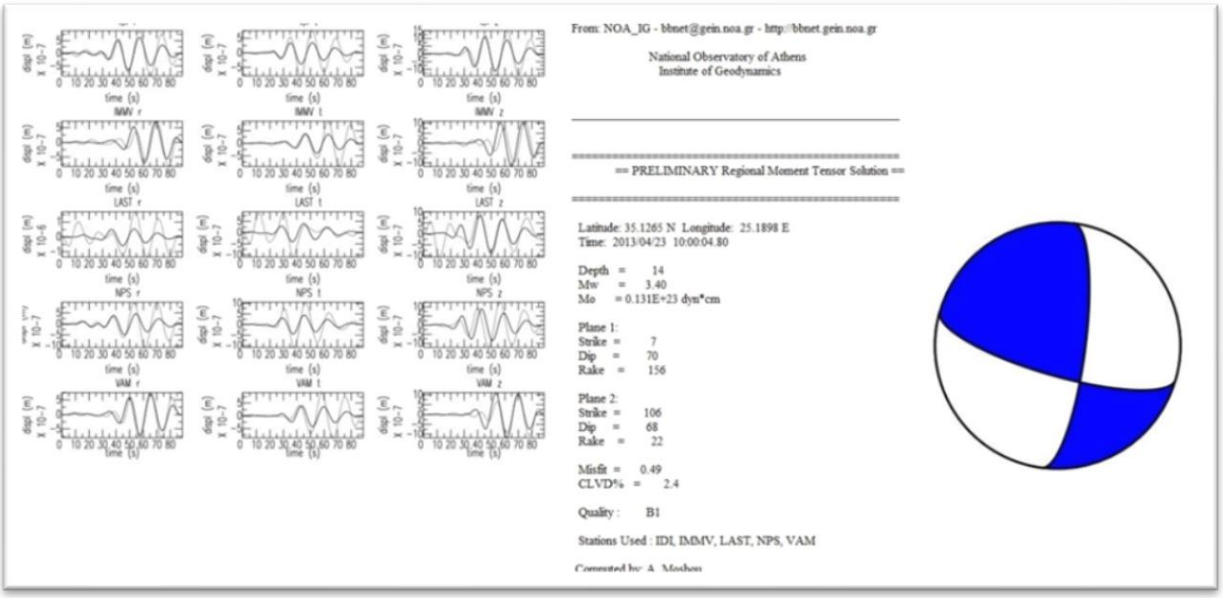
From: NOA_IG - bbnet@gein.noa.gr - http://bbnet.gein.noa.gr
National Observatory of Athens
Institute of Geodynamics
== PRELIMINARY Regional Moment Tensor Solution ==
Latitude: 35.1265 N Longitude: 25.1898 E
Time: 2013/04/23 10:00:04.80
Depth = 14
Mw = 3.40
Mo = 0.131E+23 dyn*cm
Plane 1:
Strike = 7
Dip = 70
Rake = 156
Plane 2:
Strike = 106
Dip = 68
Rake = 22
Misfit = 0.49
CLVD% = 2.4
Quality : B1
Stations Used : IDI, IMMV, LAST, NPS, VAM

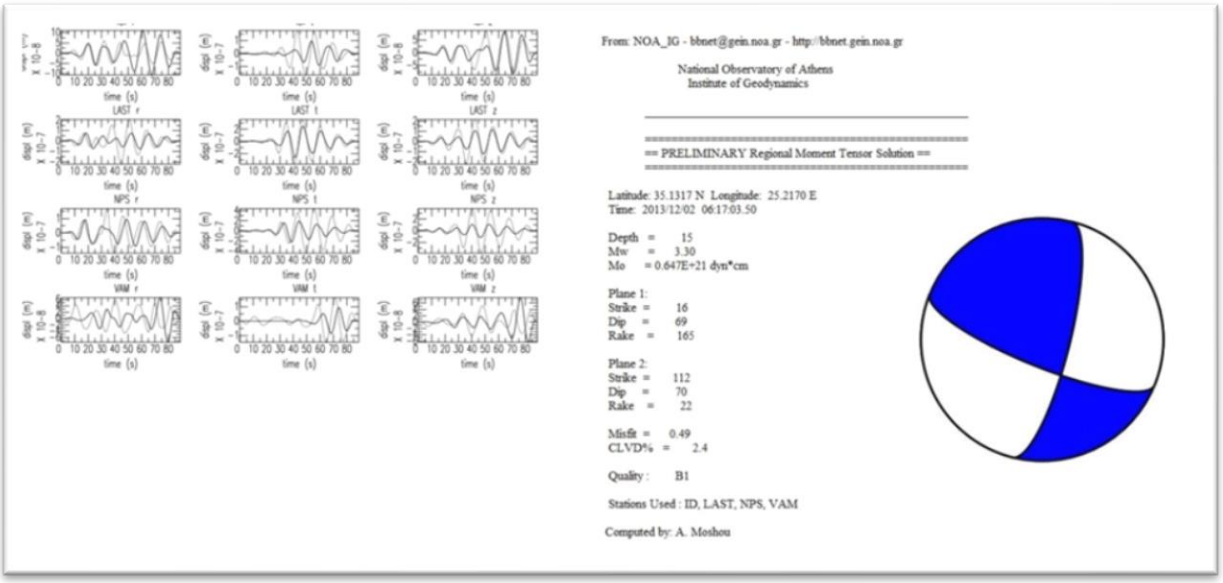
From: NOA_IG - bbnet@gein.noa.gr - http://bbnet.gein.noa.gr
National Observatory of Athens
Institute of Geodynamics
== PRELIMINARY Regional Moment Tensor Solution ==
Latitude: 35.1317 N Longitude: 25.2170 E
Time: 2013/12/02 06:17:03.50
Depth = 15
Mw = 3.30
Mo = 0.647E+21 dyn*cm
Plane 1:
Strike = 16
Dip = 69
Rake = 165
Plane 2:
Strike = 112
Dip = 70
Rake = 22
Misfit = 0.49
CLVD% = 2.4
Quality : B1
Stations Used : ID, LAST, NPS, VAM
Computed by: A. Moshou

5. Discussion – Conclusions

Our results may be used to provide new data regarding the debated orientation of crustal extension in central Crete. First, our geological mapping (Fig. 2) and the focal mechanism of the 2005 event (Fig. 6) suggest that the 6-km long Assimi – Plakiotissa fault was activated, as its location, ENE-WSW orientation, southern dip-direction and age of offset strata are compatible with seismological data. The size of the 2005 earthquake is also compatible with the length of the fault, although the fault is segmented on the earth' surface (Fig. 2) as it usually the case with geological faults (e.g. Mansfield and Cartwright, 2001; Ganas et al., 2004; see extensive discussion in Manighetti et al., 2015). The stress analysis (Fig. 5) from slip-vector data indicates a N12°W T-axis orientation which indicates a NNW-SSE extension direction.

Second, a similar extension direction is inferred 8-to-10-km further north of Assimi-Plakiotissa area, where the SE Heraklion basin (Houdetsi -Tefeli area; Fig.1; Fig. 8) hosted the 2013 seismic sequence. This latter area is characterized by a horst structure that crops out alpine rocks in the southern part of Heraklion Neogene basin (Papapetrou-Zamani, 1966; Benda et al., 1974). Two sets of north-south striking faults juxtapose the Eocene flysch of the Tripolitsa nappe with the early Serravallian fluvio-lacustrine sediments of the *Viannos* formation (Vidakis et al, 1994). The faults constitute a large tectonic zone that extents further to the north of the area of Giouchtas mountain. The horst is limited to the north and south by a set of two smaller normal faults that develop along the northwest-southeast orientation, which appear to truncate the two north-south trending faults (Fassoulas, 2001). The western bounding fault of the horst is well exposed along the highway from Houdetsi to Ligortinos. A fault scarp dipping with 75°-80° to the west occurs with well-preserved slickensides, steps and corrugations that indicate a nearly horizontal east-west trending tensional axis (Fassoulas, 2001; Fig. 1).

We applied a probabilistic non-linear earthquake relocation algorithm to obtain a high-precision pattern of the 2013 earthquakes. We obtain N-S patterns of events in map view and a depth distribution of events showing a near-vertical fault. It is suggested that the eastern bounding fault of the Houdetsi-Tefeli horst, named-here Amourgeles fault, was probably activated during the 2013 sequence because the spatial distribution of the relocated events fit to its geometry. In particular, a) the map extent of the relocated events indicates an alignment along the Amourgeles fault (Fig. 8), b) the depth-distribution seen in the cross section (Fig. 9), indicates the probable activation of a near-vertical fault whose surface projection coincides with Amourgeles fault. The east-dip direction of the proposed fault is also in agreement with the moment tensor

inversion solutions (Table 2; Fig. 12). Nevertheless, it should be noted that due to the sparse seismological network, location errors are not negligible and thus more data are needed to confirm that Amourgeles fault is active.

Furthermore, because of the N-S alignment of the 2013 events (Fig. 8) we associate the nodal plane 1 of the focal plane solutions (see Table 2) with the strike of the seismic fault. This implies that the 2013 sequence occurred along a right-lateral strike-slip fault, dipping to the east. This result further implies that the orientation of the minimum principal stress (σ_3) is constrained by the position of the compressional quadrants (colour-filled blue in Fig. 12). In other words, the 2013 sequence provides evidence of a NW-SE crustal extensional regime at the southern margin of Heraklion basin, about 20 km west of Kasteli Fault that is also accommodating NW-SE extensional strain (Fassoulas, 2001; Caputo et al., 2010; Fig. 1).

It is notable that the south margin of Heraklion basin (including part of eastern Messara) accommodates NW-SE extensional strain by the synchronous activation of normal and N-S strike-slip faults. Such a tectonic regime has been also observed across the south Aegean Sea and has been documented from both seismic and geological data (e.g. Angelier et al., 1982; Feuillet, 2013; Kiratzi, 2013; Konstantinou et al., 2016; Nomikou et al., 2017).

6. Acknowledgements

This research was funded by the GSRT bilateral project Greece – Slovenia 2005-2007 and by project ASPIDA "*Infrastructure Upgrade for Seismic Protection of the Country and Strengthen Service Excellence through Action*", project MIS-448326, implemented under the Action "*Development Proposals for Research Bodies-KRIPIS*." We used seismic phases from NOA and TEI Crete (Chania) to relocate the 2013 earthquake sequence. Some figures were prepared by use of GMT software http://gmt.soest.hawaii.edu/home . We thank Efthimios Sokos, Ilias Papadopoulos and George Drakatos for comments. We thank two reviewers for their thorough reviews which significantly improved the quality of the publication.

7. References

Allmendinger R.W., 2001. FaultKinWin, Version 1.1. A program for analyzing fault slip data for Windows™ Computers.

Angelier, J., N. Lyberis, X. Le Pichon, E. Barrier, P. Huchon., 1982. The tectonic development of the Hellenic arc and the Sea of Crete: a synthesis Tectonophysics, 86, 159-196.

Becker D., Meier T., Bohnhoff M., Harjes H.-P., 2010. Seismicity at the convergent plate boundary offshore Crete, Greece, observed by an amphibian network. Journal of Seismology, 14, 2, 369-392.

Benda, L., Meulenkamp, J.E., Zachariasse, W.J., 1974. Biostratigraphic correlations in the eastern Mediterranean Neogene. Part I: Correlation between planktonic foraminiferal, uvigerinid, sporomorphal and mammal zonations of the Cretan and Italian Neogene. Newsl. Stratigr 3, 205-217.

Caputo, R., S Catalano, C. Monaco, G. Romagnoli, G. Tortorici, L. Tortorici., 2010. Active faulting on the island of Crete (Greece), Geophysical Journal International 183 (1), 111-126.

Delibasis, N., Drakopoulos, J. K., Fytrolakis, N., Katsi-katsos, G., Makropoulos, K.C. and Zamani, A., 1981. Seismotectonic Investigation of the area of Crete Island, Proc. of the Intern. Symp. on the Hel-lenic Arc and Trench (H.E.A.T.), 1, 121-138, Athens.

Drakopoulos, J.K., Fytrolakis, N., Delibasis, N. and Makropoulos, K.C., 1983. Seismotectonic Map of the area of Crete Island with explanatory text of 26 pp., Publ. by the Techn. Chamb. Crete.

Fassoulas C., 2001. The tectonic development of a Neogene basin at the leading edge of the active European margin: the Heraklion basin, Crete, Greece. Journal of Geodynamics 31, 49-70.

Feuillet, N., 2013. The 2011–2012 unrest at Santorini rift: Stress interaction between active faulting and volcanism, Geophys. Res. Lett., 40, 3532–3537, doi:10.1002/grl.50516.

Ganas, A., et al., 2004. Active Fault Geometry and Kinematics in Parnitha Mountain, Attica, Greece. Journal of Structural Geology, 26, 2103-2118.

Ganas, A. and Parsons, T., 2009. Three-dimensional model of Hellenic Arc deformation and origin of the Cretan uplift. J. Geophys. Research 114(B6), 1–14.

Ganas A., Palyvos N., Mavrikas G., Kollias S., and Tsimi C., 2010. Geomorphological and geological observations at the coast of Tripiti hill (Heraklion harbour, Crete), in

relation to reported active faulting. Proceedings of the XIX CBGA Congress, Thessaloniki, Greece, volume 99, 11-20.

Ganas, A, N, Palyvos, G, Mavrikas, V, Karastathis, G, Drakatos, and K, Makropoulos., 2011. Recognition and Characterisation of Neotectonic Faults in Heraklion City area (Crete, Greece): a multidisciplinary approach. Geophysical Research Abstracts, Vol. 13, EGU2011-4824, 2011, EGU General Assembly 2011.

Katsamangos, G. Vidakis, M., Meulenkamp, J.E., Koutsouveli, A., Ioakim, C. & Mettos, A., 1996. Geological map of Greece in 1:50000 scale - Heraklion sheet. IGME, Athens.

Kennett, B. N.L., 1983. Seismic wave propagation in Stratified Media, Cambridge: Cambridge University Press.

Kiratzi, A. A., 2013. The January 2012 earthquake sequence in the Cretan Basin, south of the Hellenic Volcanic Arc: focal mechanisms, rupture directivity and slip models, Tectonophysics, 586, 160-172. Doi: 10.1016/j.tecto.2012.11.019.

Kiratzi, A., 2016. The 16 April 2015 Mw6.1 earthquake sequence near Kasos island at the eastern Hellenic subduction zone. Bulletin of the Geological Society of Greece, 50, 1163-1173.

Konstantinou, K.I., N. Melis and K. Boukouras., 2010. Routine Regional Moment Tensor Inversion for Earthquakes in the Greek Region: The National Observatory of Athens (NOA) Database (2001 – 2006), Seismological Research Letters, 81, 5, 750 – 760.

Konstantinou, K. I., V. Mouslopoulou, W.-T. Liang, O. Heidbach, O. Oncken, and J. Suppe., 2016. Present-day crustal stress field in Greece inferred from regional-scale damped inversion of earthquake focal mechanisms, J. Geophys. Res. Solid Earth, 121, doi:10.1002/2016JB013272.

Kritsotakis M., 2009. Management of water resources in Messara basin, Crete, Greece (in Greek). Phd Thesis. Technical University of Chania, Chania, 736p.

Lomax A, Virieux J, Volant P, Berge-Thierry C., 2000. Probabilistic earthquake location in 3D and layered models. In: Thurber CH, Rabinowitz N (eds) Advances in seismic event location. Kluwer Academic, Dordrecht, Netherlands.

Makropoulos, K., Kaviris, G., Kouskouna, V., 2012. An updated and extended earthquake catalogue for Greece and adjacent areas since 1900. Nat. Hazards Earth Syst. Sci., 12, 1425-1430.

Manighetti, I., C Caulet, L. De Barros, C. Perrin, F Cappa, and Y. Gaudemer., 2015. Generic along-strike segmentation of Afar normal faults, East Africa: Implications on fault growth and stress heterogeneity on seismogenic fault planes. Geochemistry, Geophysics, Geosystems, 16 (2), 443-467.

Mansfield, C., and J. Cartwright., 2001. Fault growth by linkage: Observations and implications from analogue models, J. Struct. Geol., 23(5), 745–763.

Mason, J. et al., 2016. A multidisciplinary investigation at the Lastros-Sfaka graben, Crete. Bulletin of the Geological Society of Greece, 50, 85-93.

Meulenkamp, J.E., Dermitzakis, M., Georgiadou-Dikeoulia, E., Jonkers, H.A., Boeger, H., 1979. Field Guide to the Neogene of Crete, Series A, 32. Pubs Geol. & Paleont. Dep., Univ. Athens, Athens.

Meulenkamp, J.E., vander Zwaan, G.J., van Wamel, W.A., 1994. On late Miocene to recent vertical motions in the Cretan segment of the Hellenic arc. Tectonophysics, 234, 53–72.

Papadimitriou, E., Karakostas, V., Mesimeri, M. & Vallianatos, F., 2016. The Mw6.7 12 October 2013 western Hellenic Arc main shock and its aftershock sequence: implications of the slab properties. International Journal Earth Sciences, DOI 10.1007/s00531–016–1294–3.

Papanikolaou, D and Nomikou P., 1998. Neotectonic blocks and planation surfaces in Iraklion Basin, Crete, Greece. Bull. Geol. Soc. Greece, XXXII/1, 231-239.

Papapetrou-Zamani, A., 1966. Contribution to the Neogene knowledge of the Heraklion area, Crete. Ann. Geol. Pays Hellen., 16, 207-232.

Papavassiliou C., Bonneau M., Katsikatsos G., 1984. Geological map of Greece in 1:50000 scale - Akhedhrias sheet. IGME, Athens.

Papavassiliou C., Bonneau M., Jonkers H.A., Meulenkamp J.E., Katsikatsos G., 1984. Geological map of Greece in 1:50,000 scale - Timbakion sheet. IGME, Athens.

Papazachos, C.B., 1998. Crustal P- and S-velocity structure of the Serbomacedonian Massif (Northern Greece) obtained by non-linear inversion of traveltimes. Geophys. J. Int., 134, 25-39. doi:10.1046/j.1365-246x.1998.00558.x.

Peterek, A., & Schwarze, J., 2004. Architecture and Late Pliocene to recent evolution of outer-arc basins of the Hellenic subduction zone (south–central Crete, Greece). J. Geodyn. 38, 19–55.

Randal, G.E., 1994. Efficient calculation of complete differential seismograms for laterally homogeneous earth models, Geophysical Journal International 118, 245 – 254.

Sokos, E. N., Zahradnik, J., 2008. ISOLA a Fortran code and a Matlab GUI to perform multiple-point source inversion of seismic data, Computers & Geosciences, 34, 8, 967-977, ISSN 0098-3004, DOI: 10.1016/j.cageo.2007.07.005.

Tarantola, A., Valette, B., 1982. Inverse problems = Quest for information. J. Geophys. Res. 50, 159–170.

Ten Veen J.H., Meijer P. Th., 1998. Late Miocene to Recent tectonic evolution of Crete (Greece): geological observations and model analysis. Tectonophysics 298, 191-208.

Ten Veen, J.H., Kleinspehn, K.L., 2003. Incipient continental collision and plate-boundary curvature: Late Pliocene – Holocene transtensional Hellenic forearc, Crete, Greece. J. Geol. Soc. (Lond.) 160, 161–181.

Vidakis M., Jonkers A., Meulenkamp J.E., and Skourtsi-Koronaiou V., 1994. Geological Map of Greece in 1:50000 scale – Archanae Sheet. IGME, Athens.

Vidakis M., Meulenkamp J.E., Koutsouveli A., Ioakim Ch., Papazeti E. and Skourtsi-Koronaiou V., 1996. Geological Map of Greece in 1:50000 scale – Heraklion Sheet. IGME, Athens.

Zygouri, V., Koukouvelas, I., & Ganas, A., 2016. Palaeoseismological analysis of the east Giouchtas fault, Heraklion basin, Crete (preliminary results). Bulletin of the Geological Society of Greece, 50, 563-571.